

Supplementary Material

Label-free Rapid Viable Enrichment of Circulating Tumor Cell by Photosensitive Polymer-based Tapered-slit Membrane Filter

Yoon-Tae Kang¹, Il Doh^{1,#}, Jiyoung Byun¹, Hee Jin Chang^{2,}, and Young-Ho Cho^{1,*}*

Contents

S1. The manual mode of circulating tumor cell isolation.....	S-2
S2. The capturing performance of the device depending on sample flow rates.....	S-3
S3. Theoretical analysis of present microfilter device.....	S-5
S4. Purity analysis of the present microfilter	S-8
S5. Release rate of the present microfilter.....	S-9
S6. Immunostaining of circulating tumor cells on the present microfilter.....	S-10
S7. Comparison between previous microfilters and the present microfilter.....	S-11
Supplementary table	S-13
Reference	S-14

S1. The manual mode of circulating tumor cell isolation

We examined the possibility of our device in circulating tumor cell isolation in manual mode. The 9ml of the prepared sample including cancer cells was withdrawn in commercial syringe, then interconnected to the zig containing the microfilter. Then we manually injected the syringe and blood sample was passed through the microfilter. The sample processing was completed within few minutes (~300ml/h) and considerable amount of cells was captured in manual mode of the present device. From the capturing performance verification using model samples, we confirmed that the present device captures 29.3% and 42.3% of A549G and DLD-1G, respectively, in manual mode. The capturing performance change of the device depending on flow rates are summarized in section S2.

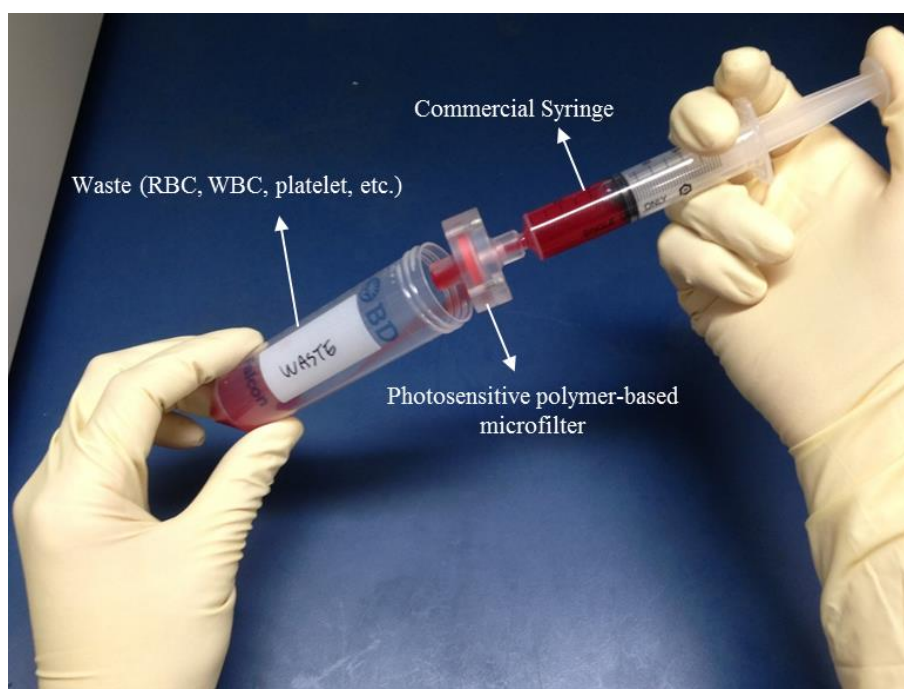


Figure S1. Photograph of the present label-free rapid viable circulating tumor cell isolation device connected to commercial syringe for manual use.

S2. The capturing performance of the device depending on sample flow rates

We verified the capturing performance of the present device depending on sample flow rates. At the flow rate of 10ml/h, the present device showed the best capturing performance; over 82% of spiked cancer cells were captured. Even at the 600% increased sample flow rate (60ml/h), we saw only 12% decrease in average capture efficiency. In addition, the result showed minimal deviation between two cell lines. However, at the flow rate of 180ml/h, the capture efficiency of A549G (lung) was significantly decreased while that of DLD-1G (colorectal) maintained over 60%. So from this experiment, we concluded that the present device can process the sample at the 10-60ml/h of flow rate, and we processed the clinical samples at the 10-60ml/h. For the manual mode (equipment-free setting), we confirmed that over 35% of captured cancer cells were successfully isolated from the device.

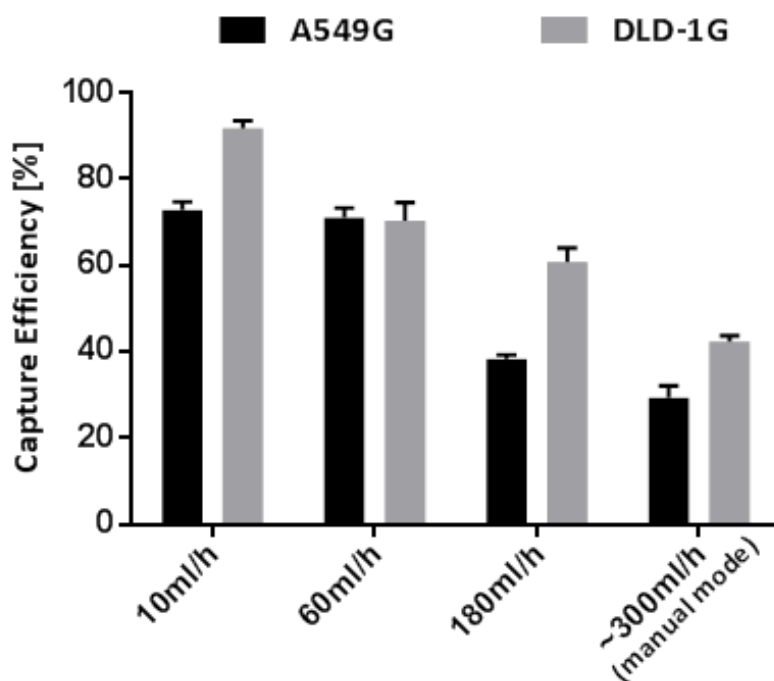


Figure S2. The capture efficiency of the A549G and DLD-1G cells depending on the sample flow rate

Table S1. The capture efficiency of the present microfilter

Flow rate	Capture efficiency		
	A549G	DLD-1G	Average
10ml/h	72.88±1.85	91.70±1.80	82.29±10.97
60ml/h	71.04±2.30	70.41±4.10	70.72±2.99
180ml/h	38.32±0.93	60.80±3.25	49.56±12.50
~300ml/h (manual mode)	29.28±2.86	42.28±1.41	35.78±7.40

S3. Theoretical analysis of present microfilter device

In order to examine the possibility of selective isolation for circulating tumor cells, we have adopted the liquid-drop modeling. This modeling assumes that the cell is like a liquid sac with constant volume and its deformability comes from sustained cortical tension in the cell membrane.

When the cell is in quasi-static condition right before passing through the slit, the pressure different, $P_{threshold}$ can be expressed using Laplace-Young equation,

$$P_{threshold} = P_{out} - P_{in} = T_c \left(\frac{1}{R_{a1}} - \frac{1}{R_{b1}} \right)$$

where R_{a1} and R_{b1} are the in-plane radius of the induced curvature, respectively, and T_c is the cortical tension of target cells.

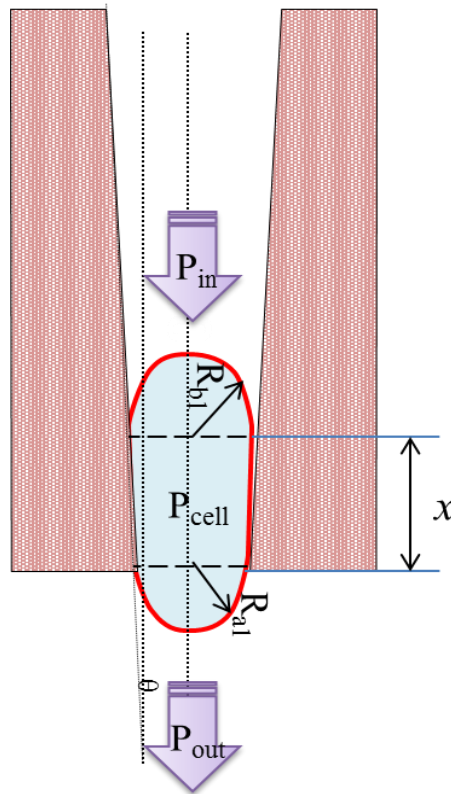


Figure S3. Theoretical model for estimation of the threshold pressure required for selective circulating tumor cell isolation in a tapered slit

Meanwhile, by conservation of the whole cell volume, deformed volume is identical to original volume, so expressed as

$$\frac{4}{3}\pi R^3 = \frac{4}{3}\pi R_{b1}^2 \frac{l}{2} \times \frac{1}{2} + \frac{4}{3}\pi R_{a1}^2 \frac{l}{2} \times \frac{1}{2} + \frac{1}{2}(2R_{b1} + 2R_{a1})l \times x$$

Where,

$$R_{b1} = R_{a1} + x \tan \theta$$

R=cell radius

$$R_{a1} = W_{out}/2$$

$l = \text{outlet height, } H$

From these relations and substitution, it can be expressed as quadratic equation of x with fixed values. In this device, we set θ as 2° and W_{out} as $6\mu\text{m}$. For cortical tension for each cells, we approximated that cortical tension of leukocyte is $50pN\mu\text{m}^{-1}$ and circulating tumor cells is $200pN\mu\text{m}^{-1}$ based on premeasured cortical tension for neutrophils ($37pN\mu\text{m}^{-1}$) and lymphoma cell ($185pN\mu\text{m}^{-1}$).^[R1] From this calculation, we verified that the threshold pressure for each cells is remarkably different, which means selective isolation for cancer cells from the leukocyte having the identical size to cancer cell is theoretically possible.

For the simplification, we fixed the critical design criteria, such as outlet width and angle of slit, then calculated the threshold pressures for each cells. However, we can further optimize our design of device by using the verified cortical tension of cancer cell and its diameter. In addition, those data measured by the circulating tumor cell isolated from the clinical sample would be the powerful background for further optimization.

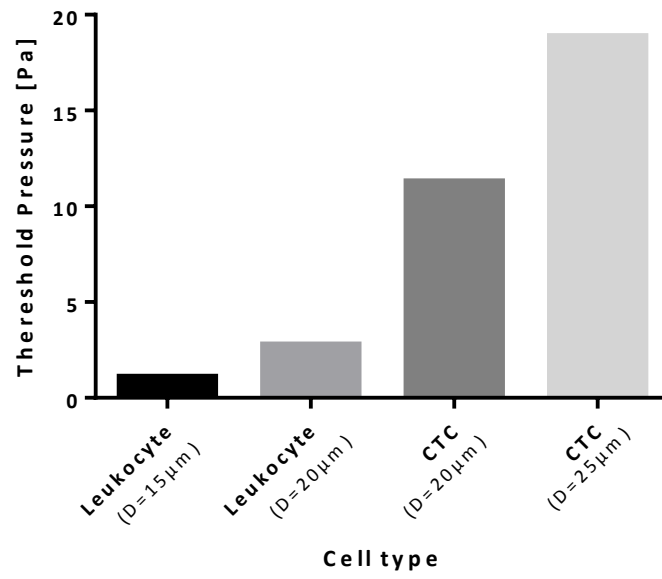


Figure S4. The estimated threshold pressure required for each cells in the present tapered-slit

S4. Purity analysis of the present microfilter

In order to verify the performance of the present filter, purity analysis was additionally performed. The colorectal cancer cell, SW620 was spiked in the whole blood at the cell concentration of 200cells/ml, and the prepared sample was processed by the present filter. After sample processing, all captured cells were released from the device and cytopinned on the slide glass and followed by immunofluorescence staining. We enumerated all DAPI positive cells and cancer cells which are cytokeratin(+)/CD45(-)/DAPI(+). The purity is defined as follows:

$$\text{Purity (\%)} = \frac{(\text{The number of the cancer cells})}{(\text{The total number of the released cells})} \times 100 (\%)$$

From this study, the purity of the present filter was 17.44 ± 7.11 %. In other words, over 17 cells out of every 100 captured and released cells were examined as the target cell (CTCs).

This purity performance is comparably lower than positive selection methods which make use of immunoaffinity between cells and antibodies (such as anti-EpCAM). However it is still comparable to previous microfilters for circulating tumor cell isolation.

Table S2. The purity analysis of the present filters using colorectal cancer cell line, SW620

	Number of the total cells (DAPI+)	Number of the target cells (CK+/CD45-/DAPI+)	Purity
A	1,022	129	12.62%
B	1,014	143	14.11%
C	621	159	25.60%

S5. Release rate of the present microfilter

The release rate of the present device was calculated as follows:

$$\text{Release rate (\%)} = \frac{(\text{The number of the released cells})}{(\text{The total number of the captured cancer cells})} \times 100 (\%)$$

As a result, the present device can release average $50.2 \pm 18.0\%$ of captured cancer cells.

Depending on the spiked cell concentration or type of cancer cells, this release rate was varied.

As it is seen in Fig. S2 (B), there are a few cancer cells still captured in the filter.

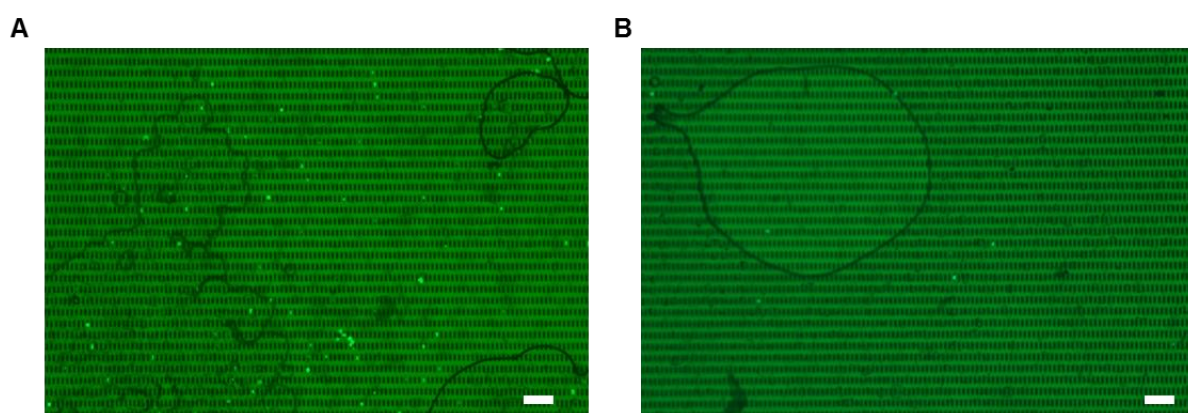


Figure S5. Fluorescent image of the captured cancer cells on the present microfilter: (A) the captured cells before cell releasing; (B) after releasing the captured cells from the microfilter.

(Scale bar=100 μ m)

S6. Immunostaining of circulating tumor cells on the present microfilter

Similar to the experiment at 2) conditions (low-concentration of non-GFP cancer cells), we tried immunostaining the circulating tumor cells from the patient samples without release. However, as it can be seen in Fig. S3, the morphology of the captured CTC was sometimes hard to define even though they express considerable level of fluorescence signal enough to identify them as a cancer cell. Thus, we conclude that the captured CTCs need to be released for careful examination of their morphologies and fluorescence signals related to proteins.

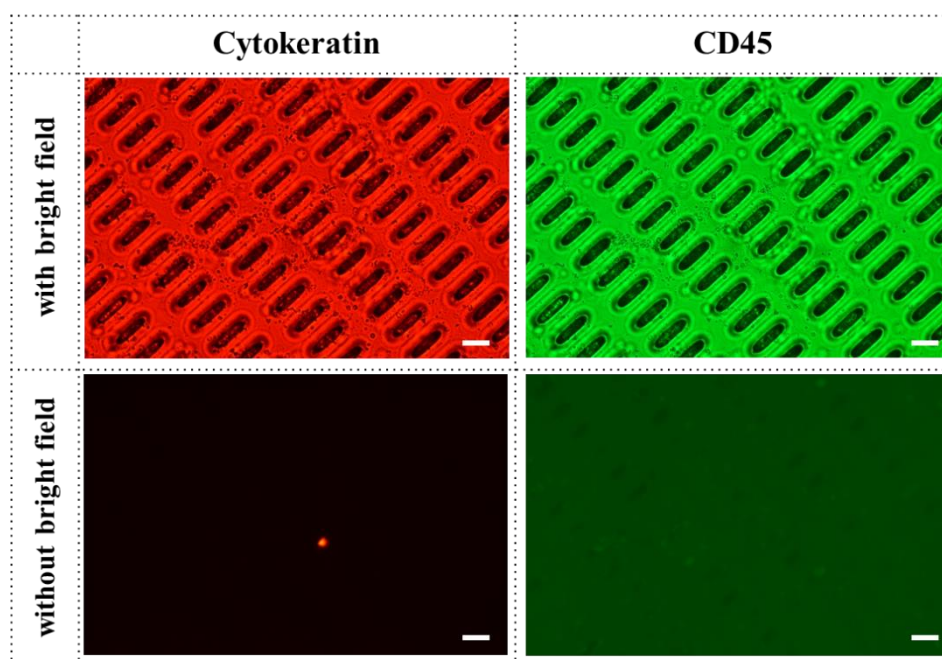


Figure S6. Immunostained circulating tumor cell of lung cancer patient (stage 4) captured on the present microfilter, imaged under fluorescence microscopy with (up) and without (down) bright field of the same position (*Scale bar*=30 μ m).

S7. Comparison between previous microfilters and the present microfilter

We compared the present microfilter with previously proposed microfilters for circulating tumor cell isolation in terms of design, experiment, and performance. Because of different sample used and processing conditions they applied, direct comparison of performance is difficult. However, when it comes to comprehensive performance verification including both model samples (9 Cancers, 11 cell lines at the 5 different cell concentration) and clinical samples (18 samples from cancer patients and 2 samples from healthy donors), the present study is superior to others. We summarized this comparison in Table S3.

Table S3. The comparison table between previous microfilter and the present microfilter for CTC isolation

	Zheng et al. [7]	Doh et al. [24]	Kang et al. [22]	Tang et al. [16]	Fan et al. [15]	Present work
Design						
Structure	Membrane with slit	Micro-pillar array	Membrane with slit	Membrane with slit	Membrane with slit	Membrane with slit
Slit shape	Straight-slit	Tapered-slit	Tapered-slit	Tapered-slit	Straight-slit	Tapered-slit
Cell line	LNCaP	H358, DLD-1	H358	MCF7, HT29, U87	A549, SK-MES-1, H446	9 cancers, 11 cell lines
Experiment (concentration)	(10-500cells/ml)	(200-500cells/ml)	(~100cells/ml)	(100cells/ml)	(100cells/ml)	(5-100cells/ml)
Clinical sample	None	None	None	15 patients, 6 healthy controls	None	18 patients, 2 healthy controls
Capture efficiency	87.3% (PBS) 89.0% (blood)	82.0% (PBS) 63.6% (blood)	89.9% (PBS) 82.4% (blood)	~95% (PBS, blood)	92% (blood)	62.5-92.4% (blood)
Throughput	~6ml/h	0.15ml/h	5 ml/h	30ml/h	10ml/h	10-30ml/h
Performance						
Viability	N/A	73.7-75.6%	72.3%	~95%	N/A	80.6%
Release efficiency	N/A	82.9%	36.0%	N/A	N/A	33.1-73.3%
CTC detection	-	-	-	0-6 CTCs	2-10 CTCs (unpublished data)	1-172 CTCs, CTC cluster
Remarks	Electrolysis on chip	-	-	-	PDMS-based microfilter	IF/IHC/RT-PCR analysis

Table S4. Measured diameter of GFP and non-GFP cell lines used for performance verification of the present microfilter.

Type	GFP cell line		Non-GFP cell line			
	lung	colorectal	lung		colorectal	
Cell line	A549G	DLD-1G	A549	H23	DLD-1	SW620
Cell diameter[μm]	27.21 \pm 3.10	29.71 \pm 7.01	20.43 \pm 2.58	24.75 \pm 4.12	27.87 \pm 3.85	22.56 \pm 4.95

Reference

[R1] Guo Q, Park S, Ma H, Microfluidic micropipette aspiration for measuring the deformability of single cells. *Lab Chip*. **2012**; 12(15): 2687-95.